



HAL
open science

Oily bioorganoclays in drilling fluids: Micro and macroscopic properties

Qiang Li, Laurence de Viguerie, Lucie Laporte, Romain Berraud-Pache,
Guangzheng Zhuang, Christelle Souprayen, Maguy Jaber

► **To cite this version:**

Qiang Li, Laurence de Viguerie, Lucie Laporte, Romain Berraud-Pache, Guangzheng Zhuang, et al.. Oily bioorganoclays in drilling fluids: Micro and macroscopic properties. Applied Clay Science, 2024, 247, pp.107186. 10.1016/j.clay.2023.107186 . hal-04443274

HAL Id: hal-04443274

<https://hal.science/hal-04443274v1>

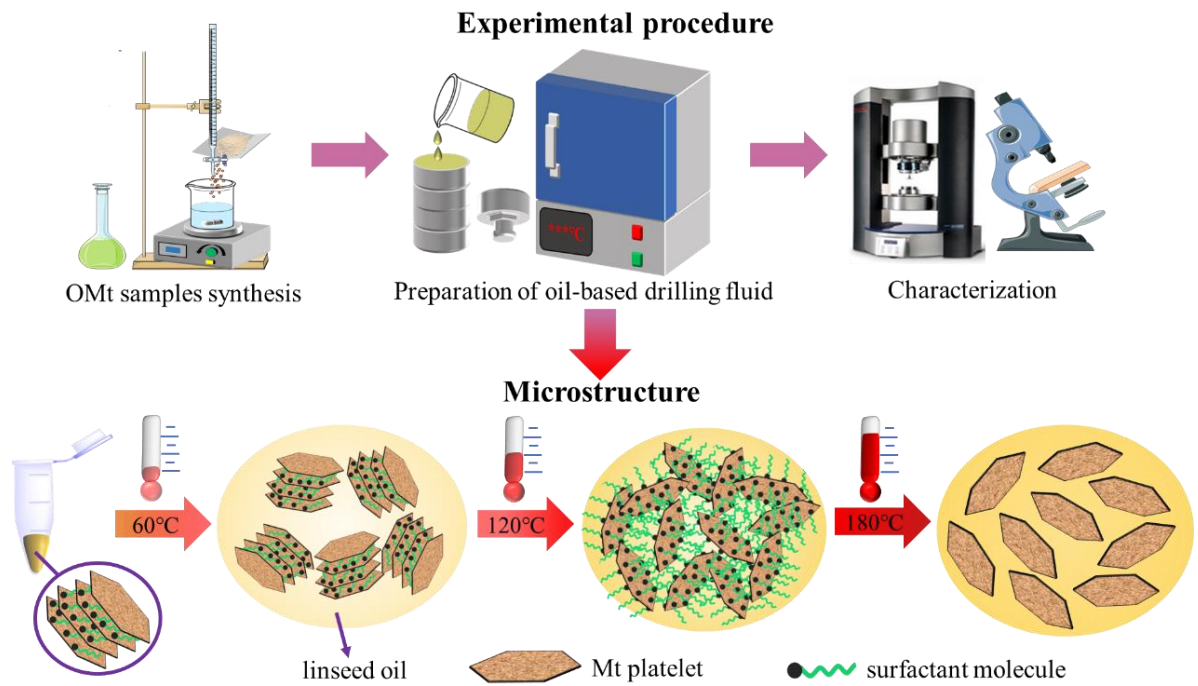
Submitted on 7 Feb 2024

HAL is a multi-disciplinary open access archive for the deposit and dissemination of scientific research documents, whether they are published or not. The documents may come from teaching and research institutions in France or abroad, or from public or private research centers.

L'archive ouverte pluridisciplinaire **HAL**, est destinée au dépôt et à la diffusion de documents scientifiques de niveau recherche, publiés ou non, émanant des établissements d'enseignement et de recherche français ou étrangers, des laboratoires publics ou privés.

23 engineering.

24 **Graphical abstract**



25

26 **Keywords:** oil-based drilling fluids; organoclay; vegetable oil; microstructure;

27 rheology; viscoelasticity

28

29

30

31

32

33

34

35

36

37

38

39 ***1. Introduction***

40 The depletion of easily accessible hydrocarbon resources has prompted the
41 petroleum industry to develop more complex and challenging reservoirs, such as
42 unconventional shales and high-temperature and high-pressure (HTHP) fields. Shale
43 reservoirs are rich in clay minerals, and various reactions will occur when exposed to
44 water-based drilling fluids, which may cause wellbore instability (Deville et al., 2011;
45 Aramendiz and Imqam, 2019). Drilling in HTHP conditions is a challenging task as
46 the harsh environments adversely affect drilling fluid performance (Zhong et al.,
47 2023). Consequently, the selection of the appropriate drilling fluids plays a pivotal
48 role in trouble-free and safe drilling operations. Oil-based drilling fluids have high
49 thermal stability and can provide low friction, shale inhibition, and salt resistance to
50 overcome some undesirable characteristics of water-based drilling fluids (Zhuang et
51 al., 2019). Therefore, oil-based drilling fluids are more suitable for shale and HTHP
52 drilling.

53 The ideal oil-based drilling fluid is a non-Newtonian fluid with appropriate
54 rheological and viscoelastic properties. Organoclays are the most important additives
55 used to adjust the colloidal and rheological properties of oil-based drilling fluids. The
56 organoclays is known for its ability to swell and form thixotropic gels in organic
57 media (Moraru, 2001). Most oil-based drilling fluids are formulated with clays
58 modified with quaternary ammonium salts, although these salts are toxic and difficult
59 to degrade. Bio-organoclays are considered to have the potential to replace traditional

60 toxic organoclays. These bio-organoclays can be obtained by modifying clay minerals
61 with biosurfactants. Phospholipids, especially lecithin, have been investigated as
62 promising candidates for the synthesis of bio-organoclays owing to their exceptional
63 zwitterionic properties (Li et al., 2023b). Lecithin is usually extracted from soybeans
64 and is mainly composed of phosphatidylcholine (PC). PC contains a choline part
65 characterized by a negatively charged phosphate group and a positively charged
66 trimethyl-amino group. It can prepare organic montmorillonite through ion-dipole
67 interactions under alkaline conditions (Li et al., 2023a).

68 The rheology of oil-based drilling fluids is not only influenced by the properties
69 and concentration of organoclays, but also affected by the composition and nature of
70 base oil (Hermoso et al., 2014). Diesel and mineral oil are common organic dispersion
71 mediums for preparing oil-based drilling fluids, but these materials will cause serious
72 pollution. The drilling cuttings contaminated with oil-based drilling fluids, drilling
73 fluid wastes and other potential contaminants pose several risks to the terrestrial,
74 aquatic and aerial environments if not disposed of properly (Pereira et al., 2022). To
75 address this problem, some eco-friendly, cheap and easily available vegetable oil such
76 as palm oil (Sulaimon et al., 2017) and soybean oil (Agwu et al., 2015) have been
77 gradually utilized as dispersion mediums in recent years.

78 The main components of most vegetable oils are triglycerides and fatty acids.
79 Some vegetable oils, referred to as siccative oils (such as linseed oil), contain
80 unsaturated fatty esters which can undergo a complex autoxidation mechanism
81 followed by crosslinking, resulting in the formation of a polymer network (Orlova et

82 al., 2021). This network structure has the ability to cure and form a solid film. The
83 curing process can be accelerated by heating or adding metallic driers (i.e. Pb^{2+} , Zn^{2+}),
84 which is a common practice in oil paints (de Viguerie et al., 2016; Artesani, 2020).
85 Zn^{2+} in the siccativ oil leads to the formation of carboxylic salts that behave as ionic
86 cross-links and act as a reinforcing site for the ionomer network (Artesani, 2020). The
87 metallic driers and siccativ oils are commonly employed in oil paints, but are rarely
88 reported in the field of oil-based drilling fluids. Additionally, temperature can have an
89 adverse impact on the performance of organoclays in oil-based drilling fluids.
90 Although previous studies have evaluated the macro-rheological properties of
91 oil-based drilling fluids at high temperatures (Patel et al., 2019b; de Brito Buriti et al.,
92 2022), the response of organoclay microstructure in oil to temperature still deserves
93 further investigation.

94 In this study, inspired by the zinc cations and siccativ oil in oil paints, the
95 biosurfactant lecithin was used to modify Mt containing Zn^{2+} to prepare organoclays,
96 which were then mixed with linseed oil to produce oil-based drilling fluid colloidal
97 systems. The microstructure of ZnOMt in mineral oil (paraffin oil) and vegetable oil
98 (linseed oil) and its effect on the rheological behavior of oil-based drilling fluids were
99 comparatively evaluated. The X-ray diffraction (XRD) and transmission electron
100 microscopy (TEM) techniques were employed to study the microstructure of ZnOMt
101 suspensions.

102 ***2. Materials and methods***

103 ***2.1 Materials***

104 The chemicals used for the synthesis of the Mt are hydrofluoric acid (40% w/w;
 105 Fluka), sodium acetate (99%; Sigma-Aldrich), magnesium acetate tetrahydrate (99%;
 106 Sigma-Aldrich), aluminium oxide (99%; Sigma-Aldrich) and silica (99.8%; DEGU).
 107 The materials used to prepare ZnOMt include: zinc acetate dihydrate (98%;
 108 Sigma-Aldrich), lecithin (94%; Sigma-Aldrich), CH₃CH₂OH (96%; Sigma-Aldrich),
 109 NaOH (1 mol/L; Sigma-Aldrich). The base oil utilized for formulating oil-based
 110 drilling fluid is categorized into two types: paraffin oil and linseed oil, both procured
 111 from Sigma-Aldrich. Their physical and chemical properties are shown in Table 1. All
 112 chemicals were used directly without additional purification.

113 Table 1 Physical and chemical properties of paraffin oil and linseed oil

	freezing point	boiling point	flash point	density	viscosity (Pa·s, 25°C)	color	main components
linseed oil	< -24 °C	>316 °C	>113 °C	0.93 g/ml at 25 °C	0.05	yellow	triglycerides
paraffin oil	< -15 °C	260~450 °C	>215 °C	0.83~0.89 g/ml at 20 °C	0.13	colorless	higher alkanes

114 2.2 Synthesis of Mt

115 The Mt employed in this work was synthesized according to the previous method
 116 (Jaber and Miéché-Brendlé, 2005; de Oliveira et al., 2021) and had the ideal formula
 117 per half unit cell: Na_{0.4}[Si₄Al_{1.6}Mg_{0.4}O₁₀(OH, F)₂]. The solution is obtained by adding
 118 the reagents in the following order: deionized water (65.61g: 3.65mol), hydrofluoric
 119 acid (0.81g: 2.02mmol), sodium acetate (0.32g: 3.90mmol), magnesium acetate
 120 tetrahydrate (0.86g: 4.01mmol), aluminium oxide (1.11g: 10.89mmol) and silica
 121 (2.42g: 0.04mol). The initial hydrogel was continuously stirred at 25°C for 4.0h and
 122 then transferred to an autoclave and heated at 190°C for 7days. The autoclave was

123 cooled to room temperature and the product was thoroughly washed with distilled
124 water and centrifuged. Finally, the synthesized Mt was dried at 60°C for 48h. The
125 cation exchange capacity (CEC) of the synthesized Mt is 130meq/100g.

126 ***2.3 Synthesis of ZnOMt***

127 The Mt structure are negatively charged due to isomorphic substitution, resulting
128 in the presence of exchangeable hydrated cations in the interlayer space to neutralize
129 the negative charges (Malamis and Katsou, 2013). This property of Mt makes it easy
130 to exchange interlayer cations with other metal cations in solution to prepare Mt
131 containing different interlayer cations. This practice has been reported in numerous
132 literatures (Yan and Zhang, 2021). To ensure that Na⁺ in the Mt is completely replaced
133 by Zn²⁺, Mt was dispersed in 5.0CEC of zinc acetate solutions for 12h under magnetic
134 stirring at 25°C. Then, the obtained mixture solution was centrifuged, and the same
135 process was repeated twice. Finally, the sample was dried in an oven at 60°C for 48h.
136 The sample will be designated as ZnMt.

137 The preparation of ZnOMt was performed using the following procedure: 2g of
138 ZnMt was dispersed in 100mL of distilled water and stirred for 2h. 1.0CEC of lecithin
139 was dissolved in 100mL ethanol and stirred for 2h. Next, the lecithin solution was
140 slowly added to the ZnMt dispersion and then NaOH was added dropwise to confirm
141 that the pH of the mixture solution was 9.0. The mixture suspension was sonicated 5
142 min and stirred 2h at 60°C, and then the suspension was centrifuged, washed 3 times
143 with 1:1 ethanol-distilled water solution, and the resulting precipitate was dried in an
144 oven at 60°C for 48h.

145 **2.4 Preparation of oil-based drilling fluid**

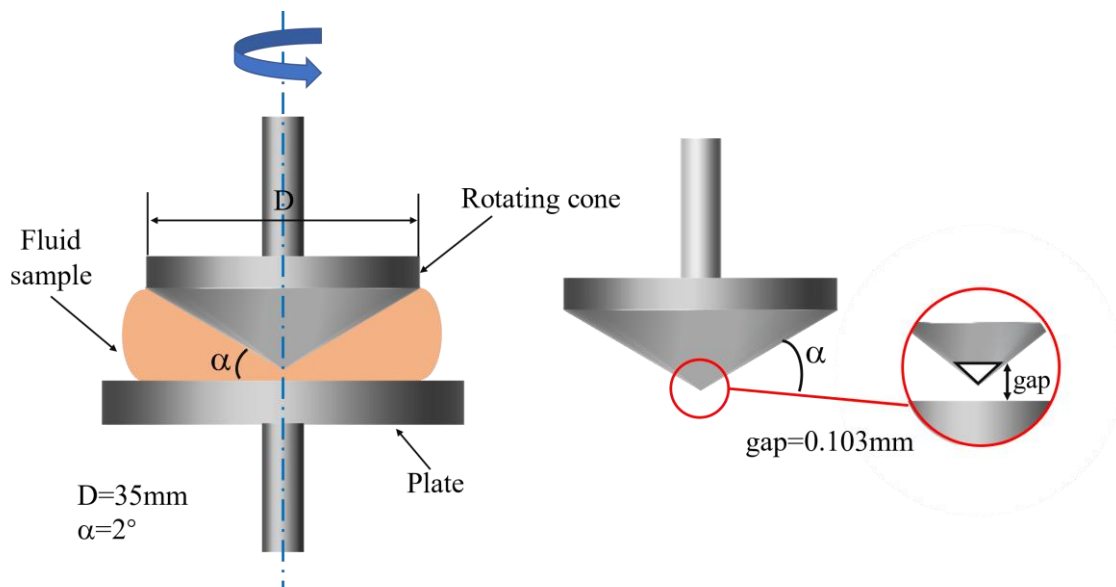
146 ZnOMt powder was added to paraffin oil and linseed oil, respectively, and stirred
147 for 1h to prepare oil-based drilling fluid with a concentration of 50kg/m³. The drilling
148 fluids should be aged at different temperatures to simulate the effect of formation
149 temperature on drilling fluid properties during drilling operations. The resulting fluid
150 was placed in a rotary oven heated to 60°C, 120°C, 180°C and kept for 16h. All the
151 procedures follow the standards of American Petroleum Institute (API), i.e., API RP
152 13D-2017 and API RP 13B-2-2018. The procedure for preparing ZnMt/oil drilling
153 fluid and Zn/oil drilling fluid is the same as that for preparing ZnOMt/oil drilling fluid.
154 The oil-based fluids were named following the template of ZnOMt/oil-temperature.
155 For example, ZnOMt/paraffin-60 is prepared with ZnOMt and paraffin oil aged at
156 60°C.

157 **2.5 Characterization**

158 The X-ray diffraction (XRD) patterns of all samples were conducted using
159 Cu-K α radiation ($\lambda=0.15406$ nm) on a Bruker D8 Advance X-ray powder
160 diffractometer, which was performed at 40 kV, 30 mA and a scanning step of 0.05°. In
161 particular, the XRD test procedure for ZnOMt/oil structure is described in detail in
162 Section 3.1. The small drop of drilling fluid was placed on copper grids covered with
163 an ultrathin carbon membrane for TEM analysis. The experiment was carried out with
164 a JEOL 1011 transmission electron microscope, operating at the accelerating voltage
165 of 100 kV (beam current around 86 μ A). The samples were imaged in Bright Field
166 (BF) mode and were examined in high vacuum mode. Optical microscopy was carried

167 out by using an Olympus BX51 microscope to obtain the dispersion of ZnOMt in oil.

168 Rheology measurements were performed with a Thermo Fisher Scientific
169 HAAKE MARS 40 rheometer, equipped with stainless steel cone plate fixtures to
170 obtain a uniform flow field. Each measurement was repeated at least twice to check
171 reproducibility. The geometry and parameters of the cone plate are shown in Fig. 1.
172 The flow curves were measured in controlled shear rate mode, with the shear rate
173 increasing linearly from 0.1s^{-1} to 1000s^{-1} in 180s. The thixotropy measurement
174 process for oil-based drilling fluid was performed according to the following
175 procedure: the shear rate linearly increased from 0.1s^{-1} to 1000s^{-1} in 180s (up-sweep),
176 and then linearly decreased from 1000s^{-1} to 0.1s^{-1} in 180s (down-sweep). The
177 calculation of the thixotropic loop area is performed using RheoWin 4.87. The
178 dynamic viscoelastic properties of the samples were collected by oscillatory rheology
179 tests. The strain amplitude sweep test from 0.1 to 100% strain was carried out at
180 $\omega=6.28\text{ rad/s}$ to evaluate the linear viscoelastic range (LVER).



181

182

Fig. 1 The geometry and parameters of the cone plate fixture

183 **2.6 Rheological Modeling**

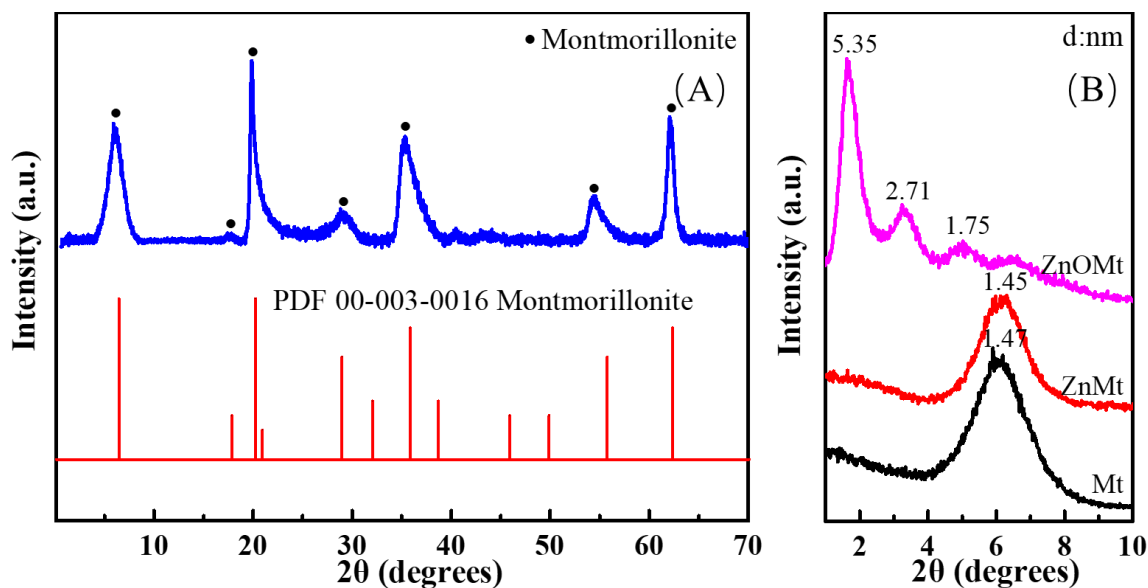
184 Rheological modeling aims to describe the flow behavior of drilling fluids
185 mathematically. The rheological modeling for drilling fluid can facilitate the
186 calculation of fluid flow dynamics (Agwu et al., 2021). Rheological models can
187 generally be divided into two groups: (i) the relationship between shear rate and shear
188 stress; (ii) the relationship between shear rate or shear stress and viscosity. In this
189 study, the rheological data of the drilling fluid at different temperatures were fitted
190 with three rheological models, including two-parameter models (i.e., Bingham-plastic,
191 Casson) and three-parameter models (i.e., Herschel-Bulkey). More details and
192 description of the rheological modeling are provided in the Supporting Information.

193 **3. Results and Discussion**

194 **3.1 X-ray diffraction**

195 The XRD patterns of the synthesized Mt and ZnOMt obtained by lecithin
196 modification are presented in Fig. 2. The XRD pattern of synthesized Mt (Fig. 2A)
197 matched well with the standard PDF card of Mt and no other reflections are observed,
198 suggesting that Mt has been successfully synthesized and has a high purity. The Mt
199 exhibited a reflection at $2\theta=6.02^\circ$ with a d_{001} -value of 1.47nm. The XRD pattern of
200 the ZnMt indicated little change in the intensity and position of the (001) reflection,
201 which is consistent with the results of previous studies (Daković et al., 2012). After
202 modification with lecithin, this reflection shifted to $2\theta=1.65^\circ$, corresponding to a basal
203 spacing of 5.35nm. The basal spacing of ZnOMt increased from 1.45nm to 5.35nm
204 (Fig. 2B), indicating the successful intercalation of lecithin into the interlayer space of

205 Mt.



206

207

Fig. 2 XRD patterns of synthesized Mt, ZnMt and ZnOMt

208

The structure of ZnOMt in oil is characterized by the XRD technique using a

209

suitable method (Fig. 3A). Firstly, a high-speed centrifuge was used to remove excess

210

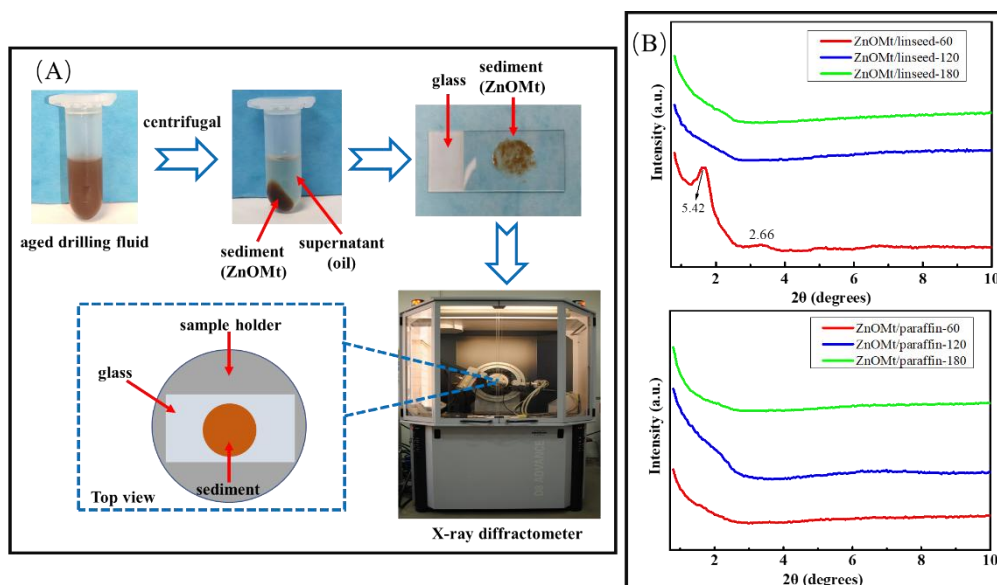
oil from the aged drilling fluid to obtain ZnOMt sediment. The ZnOMt sediment was

211

then uniformly smeared on the glass. Finally, the ZnOMt sediment can be measured

212

using the X-ray diffractometer, similar to powder samples.



213

214

Fig. 3 Interpretation diagram (A) of XRD test for ZnOMt sediment, and XRD patterns

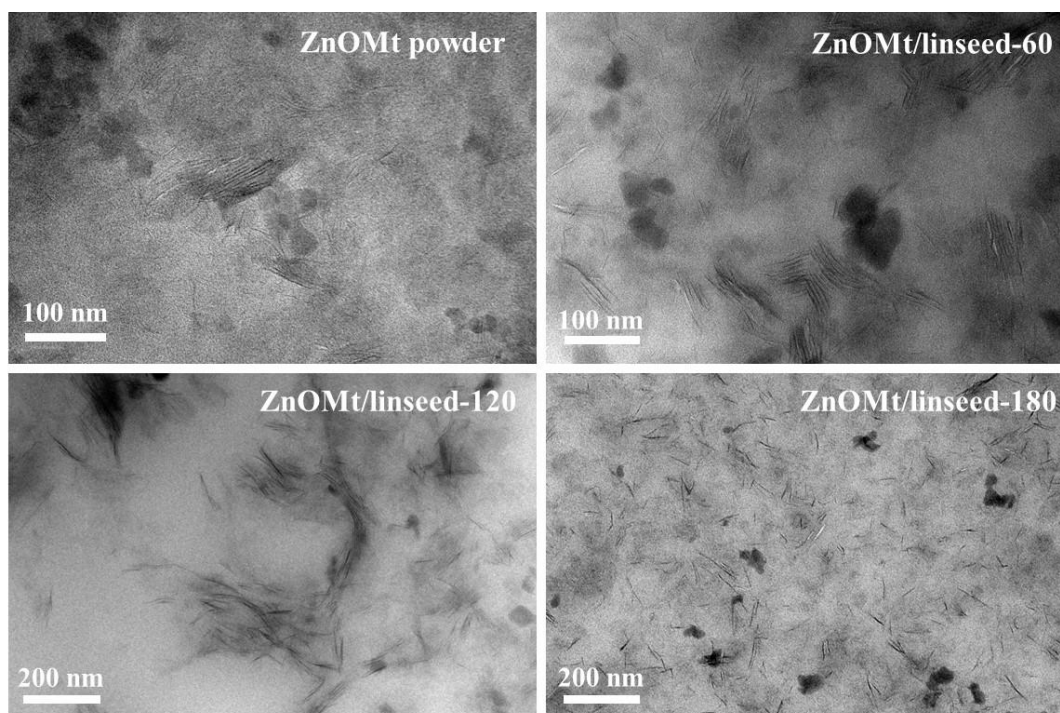
215 (B) of ZnOMt/linseed, ZnOMt/paraffin aged at different temperatures

216 The XRD patterns of ZnOMt sediment in linseed and paraffin oil aged at
217 different temperatures are presented in Fig. 3B. The base spacing of the synthesized
218 ZnOMt powder was 5.35 nm. However, the XRD results of ZnOMt/linseed and
219 ZnOMt/paraffin showed different trends after aging at various temperatures. The basal
220 spacing of ZnOMt/linseed-60 increased from 5.35 nm to 5.42 nm, suggesting the
221 penetration of oil molecules into the interlayer of ZnOMt and subsequent expansion
222 of the basal spacing. Based on previous research (Zhuang et al., 2017; Patel et al.,
223 2019a), high temperatures can promote the thermal motion of oil molecules, leading
224 to the swelling of ZnOMt in oil. There was no detectable reflection from Mt lattices in
225 the XRD patterns of ZnOMt/linseed aged at 120°C and 180°C. The same results can
226 also be observed in ZnOMt/paraffin systems. Several scholars suggested that the
227 disappearance of the (001) reflection is caused by the exfoliation of organoclays in oil
228 (Luckham and Rossi, 1999; Zhuang et al., 2016a; Zhuang et al., 2017). As the
229 temperature increased, more oil molecules intercalated into the interlayer space of the
230 ZnOMt, resulting in the exfoliation of clay platelets and reducing the attractive force
231 between Mt sheets. The exfoliated clay platelets form a “house of cards” structure
232 through three different modes of particle association : face-to-face (FF), edge-to-face
233 (EF) and edge-to-edge (EE) (van Olphen, 1964). Others believed, however, that the
234 qualitative structural information on d-spacing provided by XRD can not explain the
235 different rheological properties observed in ZnOMt/oil systems, indicating that the
236 basal spacing can not predict the fluid flow behavior (Burgentzlé et al., 2004;

237 Hermoso et al., 2014).

238 **3.2 TEM analysis**

239 In order to illustrate the microstructure of ZnOMt in oil-based drilling fluid,
240 taking the ZnOMt/linseed system as an example, the TEM images of drilling fluid at
241 different temperatures are shown in Fig. 4. The ZnOMt powder sample obtained by
242 lecithin modification exhibited a layered structure. When it was dispersed in linseed
243 oil and subjected to aging at 60°C, the layered structure remained unaltered, which is
244 consistent with the XRD results. A large number of aggregated layered ZnOMt
245 particles dispersed in the linseed oil. As the temperature increased to 120°C, the
246 ZnOMt platelets exfoliated. The exfoliated nanoclay platelets were not randomly
247 dispersed in the oil but formed compact clay tactoids and then a kind of network
248 structure was formed. The ZnOMt/linseed-180 sample was completely exfoliated but
249 presented a different dispersion state from ZnOMt/linseed-120. The ZnOMt platelets,
250 of approximately 60 nm, were homogeneously dispersed in the linseed oil, without
251 contact with each other. The network structure formed by the clay platelets was
252 destroyed, because of the degradation of the surfactant in the ZnOMt at high
253 temperature. The effect of temperature on the microstructure of ZnOMt is mainly
254 reflected in the exfoliation and the degradation of surfactants. The relationship
255 between the microstructure and rheological properties of ZnOMt in oil will be
256 explained in detail in the following sections.



257

258 Fig. 4 TEM images of ZnOMt powder, and ZnOMt/linseed aged at different

259

temperatures

260

3.3 Dispersion

261

The dispersion states of ZnOMt and ZnMt powder in paraffin oil and linseed oil

262

at different temperatures were obtained mainly by optical microscopy for observing

263

the overall size distribution of the particles. As shown in Fig. 5, the ZnMt samples

264

were not uniformly dispersed throughout the organic medium for either paraffin oil or

265

linseed oil. Due to the strong hydrophilicity of ZnMt, it is difficult for oil molecules to

266

penetrate into the interlayer space to swell the clay particles. However, it is worth

267

noting that the dispersion of ZnMt in paraffin and linseed oil is distinct. The ZnMt

268

samples were randomly dispersed in linseed oil without any contact, whereas in

269

paraffin oil they were interconnected. These particles tend to gather and partially

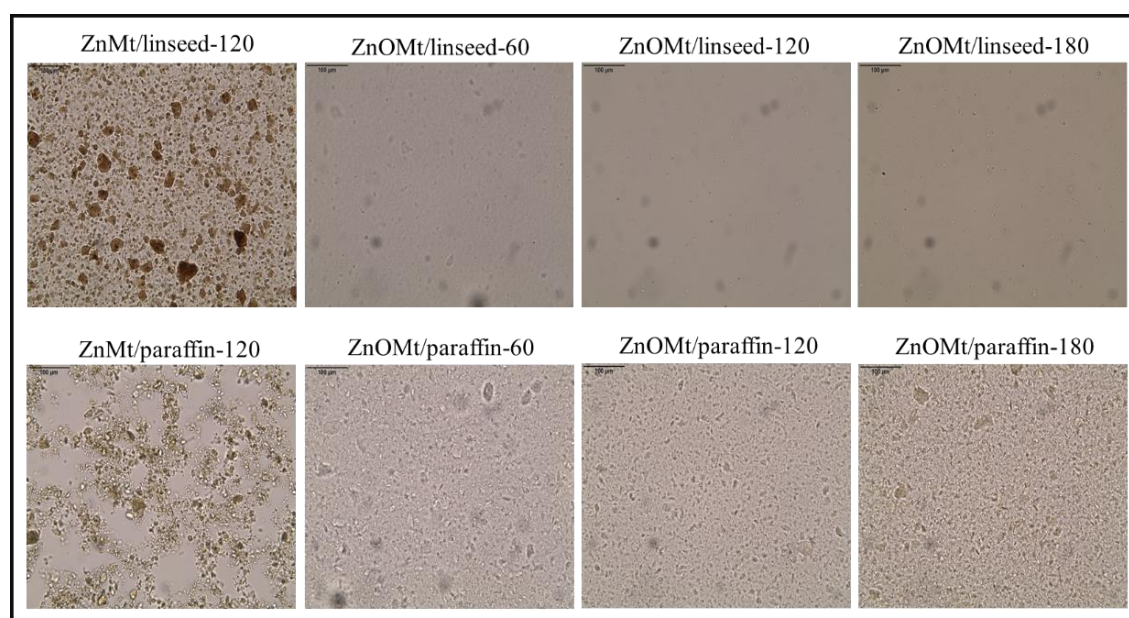
270

overlap each other and form a net-like structure. The organo-modification of ZnMt

271

with lecithin evidently improved its dispersion in oil. Although the dispersion of

272 ZnOMt in both oils was stable, the dispersion of ZnOMt in linseed oil was more
273 homogeneous and the particle size was smaller. The ZnOMt in paraffin oil presented a
274 large number of aggregated particles. In contrast, the aggregated particles in linseed
275 oil were very limited at any temperature. This is probably due to the fact that linseed
276 oil is polar compared to non-polar paraffin oil, which has a stronger affinity for
277 ZnOMt modified by polar molecules of lecithin (Jones, 1983; Ma et al., 2023). In
278 addition, temperature contributes to the dispersion of ZnOMt in oil-based drilling
279 fluids.



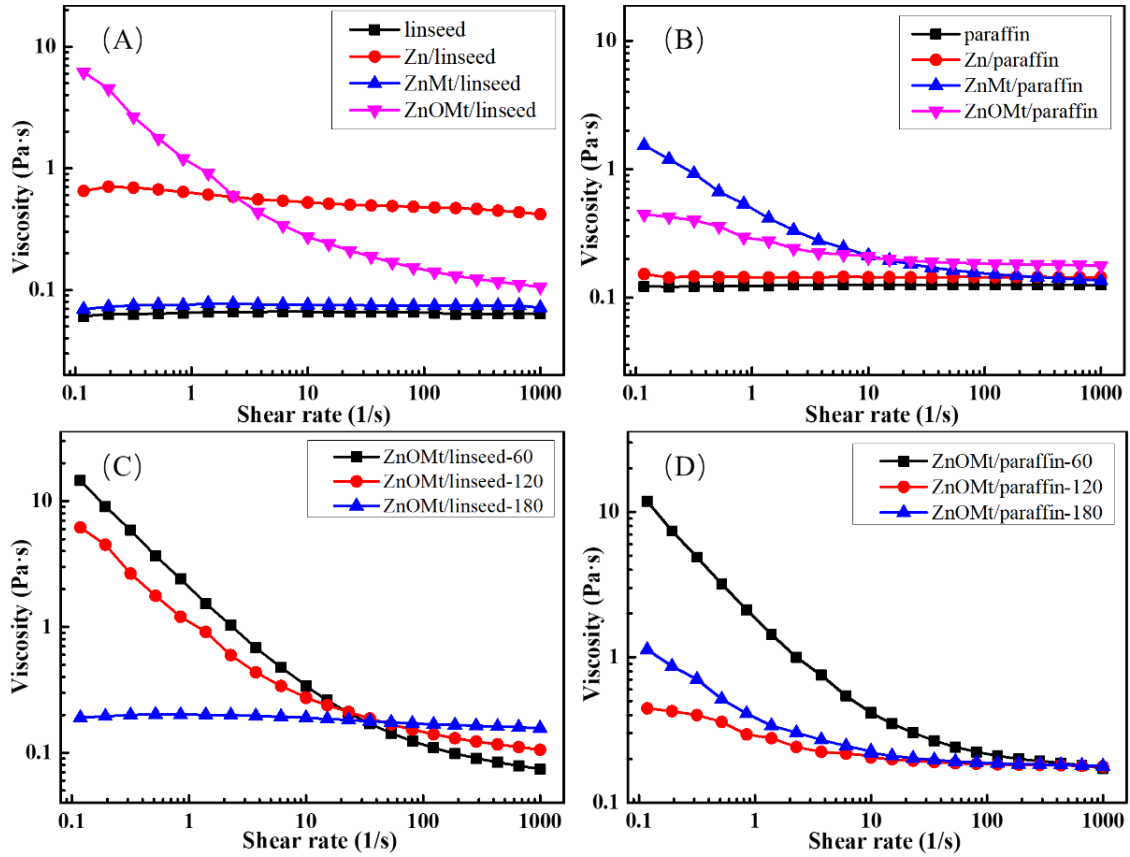
280

281 Fig. 5 Optical microscope images of ZnMt and ZnOMt in oil-based drilling fluid

282 **3.4 Rheological properties**

283 The relationship between shear stress and shear rate is the most accurate
284 description of drilling fluid flow behavior (Arain et al., 2022). Fig. 6(A, B) illustrates
285 the flow behavior of oil-based drilling fluid containing Zn^{2+} , ZnMt, ZnOMt samples
286 as a function of shear rate at 120°C: different rheological behaviors were obtained in
287 oil phases. Pure linseed and paraffin oil are Newtonian fluids, exhibiting a constant

288 viscosity at any shear rate. For linseed oil, the addition of Zn^{2+} remarkably increased
289 the viscosity of linseed oil, and the viscosity of the system grew from 0.06 to 0.5 Pa·s,
290 which may be caused by the saponification reaction between the zinc cations and the
291 esters of the siccativ oil, as commonly reported in the literature (Osmond, 2019;
292 Artesani, 2020). The addition of ZnMt had no effect on the viscosity of linseed oil,
293 while ZnOMt modified its rheological behavior from Newtonian to shear thinning: the
294 ZnOMt/linseed oil system displayed high viscosity at low shear rates and the viscosity
295 decreased with increasing shear rates, which is highly desirable in drilling operations.
296 For paraffin oil, Zn^{2+} did not affect the flow behavior of paraffin oil, as it is mainly
297 composed of alkanes that cannot react with Zn^{2+} . Interestingly, paraffin oil containing
298 ZnMt was a non-Newtonian fluid with shear thinning properties, while linseed oil
299 containing ZnMt was a Newtonian fluid. This may be due to the different dispersion
300 states of ZnMt in two oils. The net-like structure (Fig. 5) formed by ZnMt in paraffin
301 oil leads to an increase in viscosity. Conversely, the dispersion of ZnOMt in paraffin
302 oil did not yield satisfactory rheological properties. The ZnOMt showed better
303 rheological performance and application potential for drilling fluid in linseed oil
304 compared to paraffin oil.



305

306 Fig. 6 Flow tests of oil-based drilling fluids prepared by Zn^{2+} , ZnMt, ZnOMt at 120°C

307 (A, B) and flow tests of ZnOMt/oil fluids at varying temperatures (C, D)

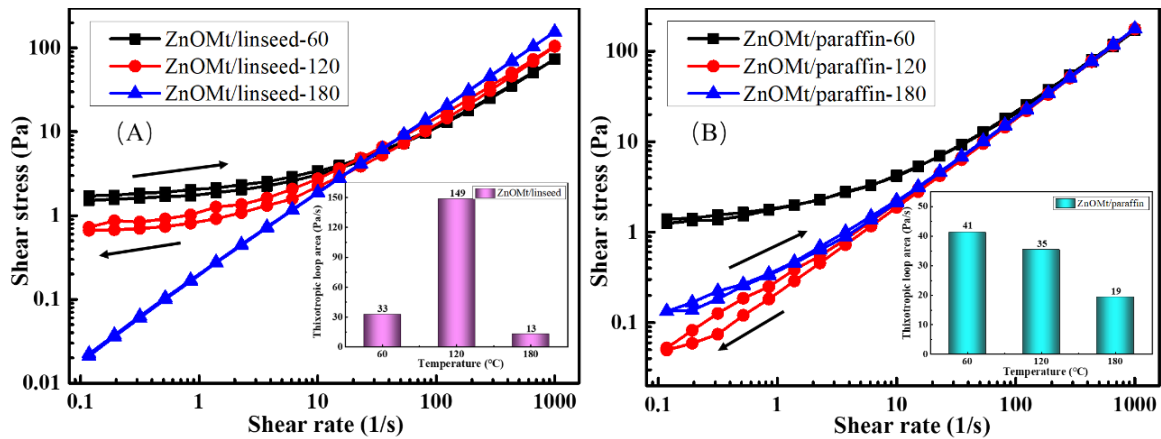
308 The rheological behavior of oil-based drilling fluid is not only affected by the oil
 309 nature, but also depends on the temperature. As shown in Fig. 6(C, D), the rheological
 310 properties of oil-based drilling fluids were altered as the temperature increased. At
 311 temperatures below 120°C, ZnOMt/linseed fluids exhibited shear thinning behavior at
 312 low shear rates. The viscosity measured at zero shear rate can be used to indicate the
 313 pumpability of drilling fluids and as a rheological parameter to evaluate barite sag,
 314 borehole cleaning, surge, and swab pressures (Maxey et al., 2008; Li et al., 2022). The
 315 viscosity of ZnOMt/linseed oil systems at low shear rates decreased gradually with
 316 increasing temperature. As the temperature increased to 180°C, the system viscosity
 317 decreased to 0.2 Pa·s and became a Newtonian fluid. This reduction may be due to the

318 fact that temperature (180°C) disrupts the structure of clay platelets and reduces the
319 connection and bonding between clay particles. The ZnOMt lost its ability to adjust
320 linseed oil-drilling fluid rheological properties at 180°C, indicating that the
321 electrochemical attraction between clay particles has totally disappeared. The
322 ZnOMt/paraffin oil system exhibited similar rheological behavior to the
323 ZnOMt/linseed oil fluid at 60°C. However, when the temperature rose to 120°C, its
324 viscosity dropped significantly and tended to exhibit the properties of Newtonian fluid.
325 Comparing the rheological properties of ZnOMt in linseed oil and paraffin oil, it can
326 be concluded that the ZnOMt/linseed oil system is more resistant to high
327 temperatures.

328 ***3.5 Thixotropy***

329 The thixotropy of the drilling fluid plays a crucial role in controlling the rate of
330 penetration at low shear rates within the well annulus and ensuring effective
331 suspension of cuttings (Celino et al., 2022). The microstructure of drilling fluid is
332 disrupted in the up-sweep, while rebuilt in the down-sweep and hysteresis is induced
333 in the flow curves. Fig. 7 illustrates the thixotropic loop curves of the ZnOMt/oil
334 system at different temperatures. The loop areas of ZnOMt/linseed-60 and
335 ZnOMt/linseed-180 fluids were minimal due to the lack of ZnOMt exfoliation at 60°C
336 and the degradation of surfactant molecules at 180°C, resulting in poor thixotropy.
337 Conversely, the loop area is higher at 120°C indicating greater thixotropy. According
338 to XRD and TEM results, this is due to the exfoliation of ZnOMt and the resulting
339 network structure in linseed oil. Based on the loop area values, the thixotropic loop

340 areas of the ZnOMt/paraffin system were not satisfactory, whatever the temperature.



341

342 Fig. 7 The thixotropic loop curves and areas of the ZnOMt/linseed (A) and

343 ZnOMt/paraffin (B) system at different temperatures

344 3.6 Rheological modeling

345 The knowledge of the drilling fluid rheological model is crucial, as the accuracy
346 of fitting the model to the actual properties of the drilling fluid will dramatically affect
347 the drilling hydraulics calculations (Wiśniowski et al., 2020). In this work, the R^2 ,
348 SSR, and RMSE are used to determine the performance of the rheological models.
349 These parameters were defined by fitting constants using regression analysis obtained
350 from rheological data. The curve fitting of the rheology model at different
351 temperatures, including the obtained rheological constants and derived statistical
352 parameters, is provided in the Supporting Information.

353 A satisfactory model to characterize the rheological properties of drilling fluids at
354 different temperatures was determined based on the values of fitted parameters such
355 as R^2 (greater than 0.99), SSR (less than 5) and RMSE (less than 0.2) (Rafieefar et al.,
356 2021). As expected, the Bingham-plastic model was not suitable for describing the
357 rheological behavior of non-Newtonian drilling fluid because the model expresses a

358 linear relationship. In comparison with the Bingham-plastic model, the Casson model
359 fitted better, revealing the nonlinear relationship between the shear stress and shear
360 rate. The Herschel-Bulkey model represents the most accurate fitting results of
361 drilling fluids at different temperatures. This is why the Herschel-Bulkley model is
362 selected for utilization in the drilling fluid field.

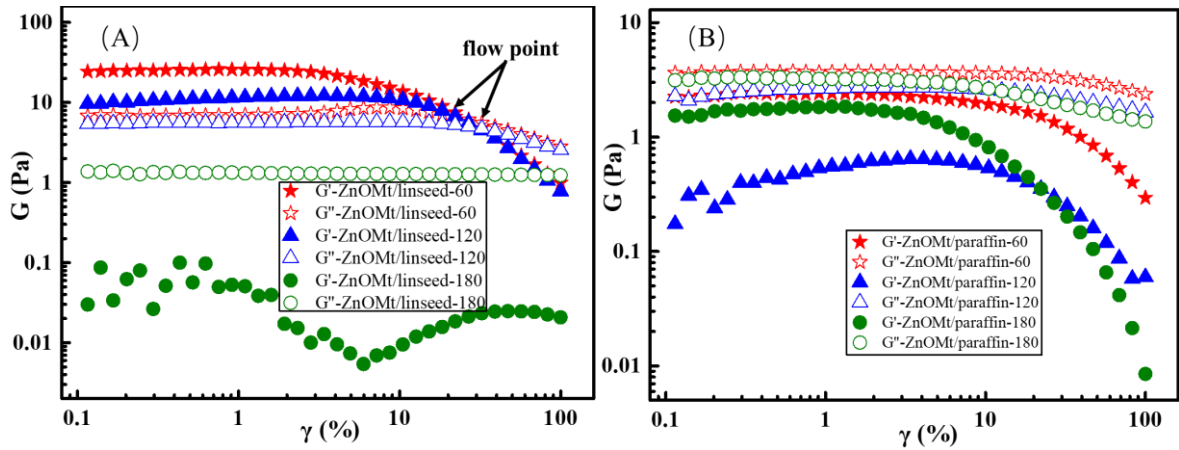
363 Rheological parameters such as flow behavior index (n) and consistency
364 coefficient (k) obtained by the Herschel-Bulkley model provide more valuable
365 information. The n value can be used to evaluate the ability of drilling fluids to carry
366 cuttings, and k is the measure of the consistency of the fluid, which is proportional to
367 the effective viscosity (Maiti et al., 2021). The drilling fluid with the lowest n value
368 and the highest k value has a greater ability to suspend and carry drill cuttings. The
369 fitting results obtained from the Herschel-Bulkley model revealed that the
370 ZnOMt/linseed system exhibited an n value of 0.8884 and a k value of 0.2263 at
371 120°C. These findings indicate that the linseed oil-based drilling fluid demonstrated
372 the most favorable rheological properties at 120°C.

373 ***3.7 Viscoelastic properties***

374 Dynamic measurements were also performed on ZnOMt/oil systems to
375 understand their structural behavior (Werner et al., 2017). The amplitude sweep tests
376 are presented in Fig. 8, indicating the viscoelastic properties (storage and loss
377 modulus) of the ZnOMt/oil system at different temperatures.

378 The linear viscoelastic range (LVER) is defined by the strain range where G' and
379 G'' are approximately constant: the limit of the LVER was 3% for ZnOMt/linseed-60

380 and 8% for ZnOMt/linseed-120, respectively. The microstructure of the drilling fluid
381 within the LVER remains intact; it is a solid-like structure as the value of G' was
382 higher than that of G'' . When the drilling fluid is subjected to greater strain after the
383 LVER, micro-cracks begin to appear, which spread throughout the drilling fluid
384 system and this behavior persists until the flow point is achieved (Medhi et al., 2021).
385 The flow point ($G'=G''$) represents the overlapping point of G' and G'' , implying a
386 transition from solid-like to liquid-like characteristics. As the strain increased after the
387 flow point, $G'<G''$ and the drilling fluid behaved more like a liquid-like and viscous
388 structure. With increasing temperature, the flow point shifted towards higher shear
389 strain. The flow points corresponding to ZnOMt/linseed-60 and ZnOMt/linseed-120
390 were 25% and 34%, respectively. Higher flow point normally related to stronger inner
391 structure and suspension capacity. At 180°C, $G'' > G'$ regardless of the applied strain,
392 indicating liquid-like behavior: the internal structure of the sample was completely
393 disrupted, which is consistent with the TEM results. The ZnOMt/paraffin systems did
394 not exhibit any viscoelasticity with G'' always greater than G' at both high and low
395 temperatures. This result suggested that ZnOMt prepared from lecithin could not
396 form a network structure in paraffin oil. The composition and nature of the base oil is
397 also an important factor in the viscoelasticity of the drilling fluid.



398

399 Fig. 8 The amplitude sweep tests of the ZnOMt/linseed (A) and ZnOMt/paraffin (B)

400

systems at different temperatures

401 3.8 Discussion of rheological mechanism

402

Based on the experimental findings, a comprehensive analysis of the impact of

403

temperature on the rheological properties of linseed oil-based drilling fluid and the

404

microstructure of ZnOMt in linseed oil is thoroughly discussed. A schematic

405

representation of the microstructure of ZnOMt in linseed oil at different temperatures

406

is proposed in Fig. 9. The synthesized ZnOMt maintained the layered structure while

407

exhibiting an increased interlayer spacing, suggesting the intercalation of lecithin.

408

This observation is further supported by the XRD and TEM results. After the

409

dispersion of ZnOMt in linseed oil at 60°C, no exfoliation has been observed. The

410

aggregation of larger clay particles impeded the flow of drilling fluid and resulted in

411

higher viscosity. In addition, the high aspect ratio of the ZnOMt further reinforced this

412

flow resistance (Cruz et al., 2019). When the temperature rose to 120°C, the oil

413

molecules intercalated into the interlayer space and caused exfoliation of the ZnOMt

414

(van Olphen, 1964; Luckham and Rossi, 1999). Lecithin molecules adsorbed on the

415

surface of ZnOMt possess long and flexible alkyl chains, which facilitated their

416 entanglement with each other, leading to a physical attraction (Zhuang et al., 2016b;
417 Liu et al., 2023). By increasing the temperature up to 180°C, lecithin molecules started
418 to degrade, and the network structure of the drilling fluid was completely destroyed.
419 The exfoliation of ZnOMt leading to its homogeneous dispersion in oil was confirmed
420 by observations using optical microscopy and TEM.

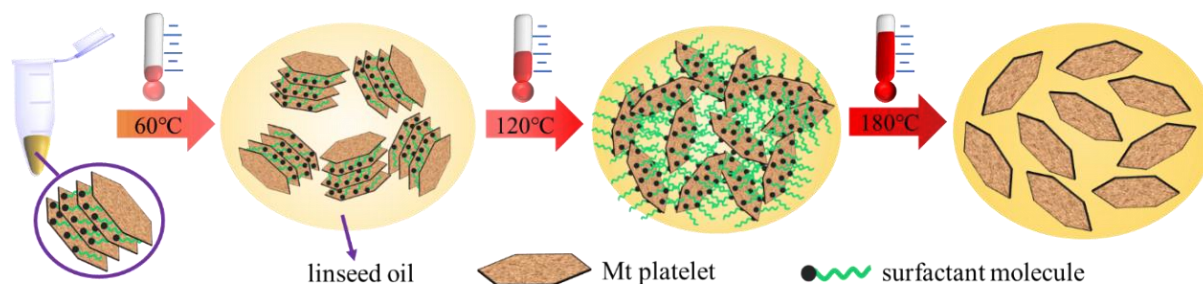


Fig. 9 The microstructure of ZnOMt in linseed oil at different temperatures

423 **4. Conclusions**

424 A systematic and in-depth experimental work was performed to probe the
425 potential of siccative oil (linseed oil) as an alternative to mineral oil-based drilling
426 fluid. The viscoelasticity, thixotropy, and microstructure of ZnOMt in linseed oil and
427 paraffin oil at different temperatures were compared and investigated. The ZnOMt
428 prepared by zinc ions and lecithin showed viscoelastic behavior in linseed oil when
429 the temperature didn't succeed 120 °C. The microstructure of ZnOMt in linseed oil
430 undergoes three stages with rising temperature: swelling→exfoliation→high
431 dispersion. The association of exfoliated clay platelets and the intertwining of
432 surfactant molecules adsorbed on the clay surface are the basis for forming a network
433 structure and thixotropy in drilling fluids. In addition, the paraffin oil-based drilling
434 fluids always displayed liquid-like behavior, while linseed oil-based drilling fluids
435 exhibited viscoelastic properties and maximum thixotropy at 120°C. The favorable

436 properties of vegetable oil-based drilling fluids containing organoclays provide great
437 potential for their application in drilling engineering.

438 *Acknowledgments*

439 Qiang Li is grateful for the scholarship (No. 202006440010) awarded by the
440 China Scholarship Council (CSC). This project was funded by the Region Ile de
441 France, DIM-MAP “Matériaux anciens et patrimoniaux” (project RheoPaint).

442 *References*

443 Agwu, O.E., Akpabio, J.U., Ekpenyong, M.E., Inyang, U.G., Asuquo, D.E., Eyoh, I.J., Adeoye,
444 O.S., 2021. A critical review of drilling mud rheological models. *Journal of Petroleum Science*
445 *and Engineering* 203, 108659.

446 Agwu, O.E., Okon, A.N., Udoh, F.D., 2015. A comparative study of diesel oil and soybean oil
447 as oil-based drilling mud. *Journal of Petroleum Engineering* 2015, 1-10.

448 Arain, A.H., Ridha, S., Mohyaldinn, M.E., Suppiah, R.R., 2022. Improving the performance of
449 invert emulsion drilling fluid using boron nitride and graphene nanoplatelets for drilling of
450 unconventional high-temperature shale formations. *Journal of Molecular Liquids* 363, 119806.

451 Aramendiz, J., Imqam, A., 2019. Water-based drilling fluid formulation using silica and
452 graphene nanoparticles for unconventional shale applications. *Journal of Petroleum Science*
453 *and Engineering* 179, 742-749.

454 Artesani, A., 2020. Zinc oxide instability in drying oil paint. *Materials Chemistry and Physics*
455 255, 123640.

456 Burgentzié, D., Duchet, J., Gérard, J., Jupin, A., Fillon, B., 2004. Solvent-based
457 nanocomposite coatings: I. Dispersion of organophilic montmorillonite in organic solvents.

458 Journal of colloid interface science 278, 26-39.

459 Celino, K.N., Fernandes, R.d.S., de Moraes, S.C., de Souza, E.A., Balaban, R.d.C., 2022.

460 Emulsion-based drilling fluids: Rheological properties preservation facing changes on the
461 temperature, pressure and dispersed phase. Journal of Molecular Liquids 352, 118753.

462 Cruz, N., Forster, J., Bobicki, E.R., 2019. Slurry rheology in mineral processing unit operations:
463 A critical review. The Canadian Journal of Chemical Engineering 97, 2102-2120.

464 Daković, A., Kragović, M., Rottinghaus, G.E., Ledoux, D.R., Butkeraitis, P., Vojislavljević, D.Z.,
465 Zarić, S.D., Stamenić, L., 2012. Preparation and characterization of zinc-exchanged
466 montmorillonite and its effectiveness as aflatoxin B1 adsorbent. Materials Chemistry and
467 Physics 137, 213-220.

468 de Brito Buriti, B.M.A., Barsosa, M.E., da Silva Buriti, J., de Melo Cartaxo, J., Ferreira, H.S., de
469 Araújo Neves, G., 2022. Modification of palygorskite with cationic and nonionic surfactants for
470 use in oil-based drilling fluids. Journal of Thermal Analysis and Calorimetry 147, 2935-2945.

471 de Oliveira, L.H., Trigueiro, P., Rigaud, B., da Silva-Filho, E.C., Osajima, J.A., Fonseca, M.G.,
472 Lambert, J.-F., Georgelin, T., Jaber, M., 2021. When RNA meets montmorillonite: Influence of
473 the pH and divalent cations. Applied Clay Science 214, 106234.

474 de Viguerie, L., Payard, P.A., Portero, E., Walter, P., Cotte, M., 2016. The drying of linseed oil
475 investigated by Fourier transform infrared spectroscopy: Historical recipes and influence of
476 lead compounds. Progress in Organic Coatings 93, 46-60.

477 Deville, J.P., Fritz, B., Jarrett, M., 2011. Development of Water-Based Drilling Fluids
478 Customized for Shale Reservoirs. SPE Drilling & Completion 26, 484-491.

479 Hermoso, J., Martinez-Boza, F., Gallegos, C., 2014. Influence of viscosity modifier nature and

480 concentration on the viscous flow behaviour of oil-based drilling fluids at high pressure.
481 Applied Clay Science 87, 14-21.

482 Jaber, M., Miéhé-Brendlé, J., 2005. Influence du milieu de synthèse sur la cristallisation de
483 saponite : proposition de mécanisme réactionnel en milieux acide et basique. Comptes
484 Rendus Chimie 8, 229-234.

485 Jones, T.R., 1983. The properties and uses of clays which swell in organic solvents. Clay
486 Minerals 18, 399-410.

487 Li, Q., Berraud-Pache, R., Souprayen, C., Jaber, M., 2023a. Intercalation of lecithin into
488 bentonite: pH dependence and intercalation mechanism. Applied Clay Science 244, 107079.

489 Li, Q., Berraud-Pache, R., Yang, Y., Souprayen, C., Jaber, M., 2023b. Biocomposites based
490 on bentonite and lecithin: An experimental approach supported by molecular dynamics.
491 Applied Clay Science 231, 106751.

492 Li, X.-L., Jiang, G.-C., Xu, Y., Deng, Z.-Q., Wang, K., 2022. A new environmentally friendly
493 water-based drilling fluids with laponite nanoparticles and polysaccharide/polypeptide
494 derivatives. Petroleum Science 19, 2959-2968.

495 Liu, S., Zhang, C., Du, J., Huang, H., Fang, S., Li, X., Duan, M., 2023. Effect of dispersants on
496 the stability of calcite in non-polar solutions. Colloids and Surfaces A: Physicochemical and
497 Engineering Aspects 672, 131730.

498 Luckham, P.F., Rossi, S., 1999. The colloidal and rheological properties of bentonite
499 suspensions. Advances in Colloid and Interface Science 82, 43-92.

500 Ma, G.-D., Zuo, H.-R., Pang, S.-Y., Duan, M., Xiong, Y., Li, X.-L., 2023. Anchoring polyamide
501 active layer to improve the thermal stability of polyacrylonitrile composite forward osmosis

502 membrane through interfacial enthalpic effect. Separation and Purification Technology 318,
503 123954.

504 Maiti, M., Bhaumik, A.K., Mandal, A., 2021. Performance of water-based drilling fluids for
505 deepwater and hydrate reservoirs: Designing and modelling studies. Petroleum Science 18,
506 1709-1728.

507 Malamis, S., Katsou, E., 2013. A review on zinc and nickel adsorption on natural and modified
508 zeolite, bentonite and vermiculite: Examination of process parameters, kinetics and isotherms.
509 Journal of Hazardous Materials 252-253, 428-461.

510 Maxey, J., Ewoldt, R., Winter, P., McKinley, G., 2008. Yield stress: what is the True value,
511 AADE Fluids Conference and Exhibition, pp. 1-10.

512 Medhi, S., Gupta, D.K., Sangwai, J.S., 2021. Impact of zinc oxide nanoparticles on the
513 rheological and fluid-loss properties, and the hydraulic performance of non-damaging drilling
514 fluid. Journal of Natural Gas Science and Engineering 88, 103834.

515 Moraru, V.N., 2001. Structure formation of alkylammonium montmorillonites in organic media.
516 Applied Clay Science 19, 11-26.

517 Orlova, Y., Harmon, R.E., Broadbelt, L.J., Iedema, P.D., 2021. Review of the kinetics and
518 simulations of linseed oil autoxidation. Progress in Organic Coatings 151, 106041.

519 Osmond, G., 2019. Zinc soaps: an overview of zinc oxide reactivity and consequences of soap
520 formation in oil-based paintings. Metal soaps in art: Conservation research, 25-46.

521 Patel, H.A., Santra, A., Thaemlitz, C.J., 2019a. Exceptional flat rheology using a synthetic
522 organic-inorganic hybrid in oil-based muds under high pressure and high temperature,
523 SPE/IADC International Drilling Conference and Exhibition. OnePetro.

524 Patel, H.A., Santra, A., Thaemlitz, C.J., 2019b. Exceptional Flat Rheology Using a Synthetic
525 Organic-Inorganic Hybrid in Oil-Based Muds Under High Pressure and High Temperature,
526 SPE/IADC International Drilling Conference and Exhibition, p. D012S020R001.

527 Pereira, L.B., Sad, C.M.S., Castro, E.V.R., Filgueiras, P.R., Lacerda, V., 2022. Environmental
528 impacts related to drilling fluid waste and treatment methods: A critical review. Fuel 310,
529 122301.

530 Rafieefar, A., Sharif, F., Hashemi, A., Bazargan, A.M., 2021. Rheological Behavior and
531 Filtration of Water-Based Drilling Fluids Containing Graphene Oxide: Experimental
532 Measurement, Mechanistic Understanding, and Modeling. ACS Omega 6, 29905-29920.

533 Sulaimon, A.A., Adeyemi, B.J., Rahimi, M., 2017. Performance enhancement of selected
534 vegetable oil as base fluid for drilling HPHT formation. Journal of Petroleum Science and
535 Engineering 152, 49-59.

536 van Olphen, H., 1964. Internal mutual flocculation in clay suspensions. Journal of Colloid
537 Science 19, 313-322.

538 Werner, B., Myrseth, V., Saasen, A., 2017. Viscoelastic properties of drilling fluids and their
539 influence on cuttings transport. Journal of Petroleum Science Engineering 156, 845-851.

540 Wiśniowski, R., Skrzypaszek, K., Małachowski, T., 2020. Selection of a Suitable Rheological
541 Model for Drilling Fluid Using Applied Numerical Methods, Energies.

542 Yan, H., Zhang, Z., 2021. Effect and mechanism of cation species on the gel properties of
543 montmorillonite. Colloids and Surfaces A: Physicochemical and Engineering Aspects 611,
544 125824.

545 Zhong, H., Guan, Y., Qiu, Z., Grady, B.P., Su, J., Huang, W., 2023. Application of carbon

546 coated bentonite composite as an ultra-high temperature filtration reducer in water-based
547 drilling fluid. *Journal of Molecular Liquids* 375, 121360.

548 Zhuang, G., Gao, J., Peng, S., Zhang, Z., 2019. Synergistically using layered and fibrous
549 organoclays to enhance the rheological properties of oil-based drilling fluids. *Applied Clay*
550 *Science* 172, 40-48.

551 Zhuang, G., Zhang, H., Wu, H., Zhang, Z., Liao, L., 2017. Influence of the surfactants' nature
552 on the structure and rheology of organo-montmorillonite in oil-based drilling fluids. *Applied*
553 *Clay Science* 135, 244-252.

554 Zhuang, G., Zhang, Z., Sun, J., Liao, L., 2016a. The structure and rheology of
555 organo-montmorillonite in oil-based system aged under different temperatures. *Applied Clay*
556 *Science* 124-125, 21-30.

557 Zhuang, G., Zhang, Z., Sun, J., Liao, L., 2016b. The structure and rheology of
558 organo-montmorillonite in oil-based system aged under different temperatures. *Applied Clay*
559 *Science* 124, 21-30.

560